International Journal of Energetic Materials and Chemical Propulsion 10(2), 107–122 (2011)

MODELING OF SELF-IGNITION, STRUCTURE, AND VELOCITY OF PROPAGATION OF THE FLAME OF HYDROGEN AZIDE

Oleg P. Korobeinichev,[1,*] Alexander A. Paletsky,[1] N.V. Budachov,[1] Tatyana A. Bolshova,[1] & Vadim D. Knyazev[2]

[1]Institute of Chemical Kinetics and Combustion Siberian Branch of the Russian Academy of Sciences, Institutskaya st., 3, Novosibirsk, 630090 Russia

[2]Department of Chemistry, The Catholic University of America, Washington, DC 20064, USA

*Address all correspondence to Oleg P. Korobeinichev E-mail: korobein@kinetics.nsc.ru

A kinetic mechanism of thermal decomposition of hydrogen azide (HN_3) has been developed. The mechanism adequately describes experimental data on the self-ignition of HN_3 and propagation velocity of HN_3 flames available in the literature. The mechanism includes 60 reactions with 15 participating species (He, H_2, H, N, NH, NH_2, NNH, NH_3, HN_3, N_3, N_2, Ar, N_2H_2, N_2H_3, and N_2H_4). For the total pressure of 50 Torr of mixtures of HN_3 with different diluents (N_2, Ar, and He), self-ignition limits of HN_3 and flame speeds were calculated using the developed mechanism. The results of modeling of the flame structure of the HN_3/N_2 and the HN_3/Ar mixtures demonstrated that, with the HN_3 concentration in the 50–100% range, the maximum temperatures in the flame front exceed thermodynamic equilibrium values by 140–610 K; i.e., super-adiabatic flame temperatures are reached. The developed mechanism can be used for modeling combustion and thermal decomposition in chemical systems containing hydrogen azide.

KEY WORDS: *hydrogen azide, modeling, flame speed, self-ignition delay, flame structure*

1. INTRODUCTION

The goal of the current study is the development of a detailed kinetic mechanism of decomposition of gaseous HN_3 on the basis of data available in the literature. Such a mechanism should be capable of reproducing low-pressure experimental results on the flame propagation velocity, flame structure, and self-ignition limits of HN_3. An additional motivation for this study is provided by hydrogen azide being a likely intermediate in the decomposition or combustion of energetic materials with high nitrogen content, such as, for example, 5-aminotetrazole. Thus, a mechanism of HN_3 decomposition can serve as a subset of more complex and detailed mechanisms in other C–H–N systems. Hydrogen azide is a chemically simple explosive. It is a binary compound (i.e., containing only two elements) and, thus, presents a convenient modeling object for studying the chemical mechanisms of decomposition, ignition, and combustion of energetic materials at the molecular level.

Hydrogen azide decomposition and related elementary reactions have been studied by a number of groups. Laffitte et al. (1965) studied HN_3/N_2 flames stabilized at the end of a tubular reactor under the conditions of 50 Torr total pressure and an initial mixture temperature of 296 K, with the HN_3 molar fraction varying from 0.3 to 1.0 These authors observed rather high values of flame propagation velocity ranging from ~2 to 10 m/ s^{-1}, depending on the percentage of hydrogen azide in the mixture. Two methods were used for determining the flame propagation velocities: that of the flame cone area and the method of a constant-volume bomb, with the respective results being close to each other. Photography was used to determine the width of the luminous flame zone, which varied from 0.5 to 0.2 mm as the HN_3 mole fraction in the mixture changed from 0.3 to 1.0. Additional experiments performed in the 50–350 Torr pressure range with a 0.3 HN_3 mole fraction demonstrated that the flame propagation velocity was independent of pressure. The same conclusion was reached by Hajal and Combourieu (1966), where HN_3/N_2 flames (66.7% HN_3) were studied at varying pressures.

In two studies (Meyer and Schumacher, 1934; Dupre et al., 1976), contact of HN_3 with the walls of a reactor vessel during experiments resulted in effects that cannot be easily accounted for in modeling. The existing experimental database of such heterogeneous effects (i.e., reactions of active species with the wall) is not of the quality that would enable their meaningful inclusion in models. As an example, the flame propagation velocity observed at 50 Torr in the mixture of HN_3 with argon (0.3/0.7) in a tubular reactor (Dupre et al., 1976) was approximately three times higher than that reported by Laffitte et al. (1965); the former rate was not reproduced in other experiments performed in the same study. In their study of non-explosive HN_3 decomposition at low pressures (30–200 Torr) and temperatures above 250°C, Meyer and Schumacher (1934) concluded that the reaction of HN_3 decomposition is catalyzed by impurities or by the wall of the vessel, and the process can easily turn into an explosion. The main products of non-explosive decomposition are NH_3 and N_2.

In Gray (1957), dependences of HN_3 self-ignition limits on temperature (470–650°C) and pressure (5–37 Torr) were determined. The measured values of the induction period prior to spontaneous ignition are approximately 0.2 s. Gray (1957) observed a factor of 2 increase in pressure during the course of the reaction, which led him to conclude that decomposition of HN_3 occurs to form H_2 and N_2 products.

A similar conclusion was made by Rozenberg et al. (1970) in their investigation of the self-ignition of pure hydrogen azide vapor at pressures in the 0.7–70 Torr range. However, when various diluting agents (such as nitrogen, argon, helium, and others) were present, formation of ammonia was detected during ignition. From the analysis of the composition of the ignition products by infrared (IR) spectroscopy and the measured pressure increase due to the reaction, Rozenberg et al. (1970) concluded that decomposition occurs along two parallel pathways: $2HN_3=H_2+3N_2$ and $3HN_3=NH_3+4N_2$. Rozenberg et al. (1970) also demonstrated that the relative ammonia yield per mole of hydrogen azide depends on the averaged temperature value, following the same dependence for all types of diluting agents except hydrogen.

Kajimoto et al. (1979) studied decomposition of HN_3 in argon in shock tube experiments performed in the pressure and temperature ranges of 600–2200 Torr and 1200–1350 K, respectively. The values of the effective decomposition constant (k_{eff}) of the $HN_3+M \rightarrow NH+N_2+M$ reaction were determined; however, contributions of the different spin states of the NH products were not distinguished. It is known that formation of the ground state $^3NH(HN_3+Ar \rightarrow NH(^3\Sigma)+N_2+Ar)$ is characteristic for the thermolysis of hydrogen azide; formation of the excited singlet NH is observed in the photolysis of HN_3. Kajimoto et al. (1979) suggested a 10-reaction mechanism of HN_3 decomposition in argon, which adequately described the HN_3 and NH profiles obtained in the experiments.

Alexander et al. (1990) performed calculations on the potential energy surface of the $HN_3+M \rightarrow N_2+NH+M$ reaction and reported values of the energy barriers for both the singlet and the triplet NH channels. The calculated energy barrier for the triplet NH channel exceeded by ~150 kJ/mol^{-1} the activation energy of 128 kJ/mol^{-1} obtained by Kajimoto et al. (1979) in their experimental kinetics study, which did not distinguish between the spin states of NH.

Le Bras and Combourieu (1973) studied the reactions between HN_3 and atomic hydrogen and nitrogen. Using their measured values of the rate constant for the HN_3+H reaction, Le Bras and Combourieu (1973) suggested that in the preheating zone at temperatures of ~1300 K, the rate of the HN_3+H reaction is higher than the rate of HN_3 decomposition. The major supply of the H atoms in the preheating zone is by their diffusion from the high-temperature flame zone, where they are present in large amounts. Thus, Le Bras and Combourieu (1973) proposed that the HN_3+H reaction is responsible for flame propagation and leads to the formation of NH_3 via the following route: $HN_3+H \rightarrow NH_2+N_2$ followed by $H+NH_2 \rightarrow NH_3$. One prediction that follows from this suggestion is that increased formation of NH_3 should be observed under lower temperature conditions (for example, those corresponding to higher concentrations of diluting agents). This prediction is in agreement with the experimental results of Rozenberg et al. (1970).

Analysis of the existing literature data indicates that there is no single mechanism capable of describing all existing experimental data on HN_3 decomposition flames obtained under varying conditions.

2. RESULTS AND DISCUSSION

2.1 Description of the Mechanism

The full mechanism proposed in this work to describe the process of HN_3 combustion and its ignition at low pressure is presented in Table 1. The mechanism consists of 60 reactions (Table 1) with the participation of 15 species: He, H_2, H, N, NH, NH_2, NNH, NH_3, HN_3, N_3, N_2, Ar, N_2H_2, N_2H_3, and N_2H_4. The thermodynamic parameters and the transport properties for most of the species were taken from Konnov (1998). The transport properties of species N_3 and HN_3 were evaluated by using Lennard-Jones coeffi-

TABLE 1: Kinetics mechanism of HN_3 decomposition [units are cm^3, mole, s, J, K; $k = A \times T^{n} \exp\left(-E_a / RT\right)$]

Number	Reaction	*A*	*n*	E_a	Reference
1	$HN_3+M=N_2+NH+M$	7.58E+14	0	151316	Kajimoto et al. (1979)
Enhanced third-body efficiency: N_2=4.0; HN_3=8.0; He=4.0; Ar=1.0					
2	$HN_3+N=N_2+NNH$	2.95E+09	0	0	Le Bras and Combourieu (1973)
3	$HN_3+H=N_2+NH_2$	1.53E+13	0	19,290	
4	$HN_3+NH=NH_2+N_3$	3.00E+11	0	6693	Kajimoto et al. (1979)
5	$HN_3+NH_2=NH_3+N_3$	6.00E+11	0	4590	-//-
6	$H+H+M=H_2+M$	6.50E+17	−1	0	Konnov and De Ruyck (2001)
Enhanced third-body efficiency: H_2=0.0					
7	$H+H+H_2=H_2+H_2$	1.00E+17	−0.6	0	-//-
8	$N_2+M=N+N+M$	1.00E+28	−3.3	942,030	-//-
Enhanced third-body efficiency: N_2=5.0					
9	$NH+M=N+H+M$	2.65E+14	0	316,100	-//-
10	$NH+H=N+H_2$	3.20E+13	0	1360	-//-
11	$NH+N=N_2+H$	9.00E+11	0.5	0	-//-
12	$NH+NH=NH_2+N$	5.95E+02	2.9	−8370	-//-
13	$NH+NH=NNH+H$	5.10E+13	0	0	-//-
14	$NH+NH=N_2+H_2$	1.00E+08	1	0	-//-
15	$NH+NH=N_2+H+H$	2.54E+13	0	0	Konnov and De Ruyck (2000)
16	$NH_2+M=NH+H+M$	3.16E+23	−2	382,670	Konnov and De Ruyck (2001)
17	$NH+H_2=NH_2+H$	1.00E+14	0	84,030	-//-
18	$NH_2+N=N_2+H+H$	6.90E+13	0	0	-//-
19	$NH_2+NH=N_2H_2+H$	1.50E+15	−0.5	0	-//-
20	$NH_2+NH=NH_3+N$	1.00E+13	0	8370	-//-
21	$NH_3+NH=NH_2+NH_2$	3.16E+14	0	112,080	-//-
22	$NH_2+NH_2=N_2H_2+H_2$	1.00E+13	0	6280	-//-
23	$NH_3+M=NH_2+H+M$	2.20E+16	0	391,340	-//-
24	$NH_3+M=NH+H_2+M$	6.30E+14	0	391,000	-//-
25	$NH_3+H=NH_2+H_2$	5.42E+05	2.4	41,530	-//-
26	$NH_3+NH_2=N_2H_3+H_2$	1.00E+11	0.5	90,430	-//-
27	$NNH=N_2+H$	3.00E+08	0	0	-//-
Declared duplicate reaction					
28	$NNH+M=N_2+H+M$	1.00E+13	0.5	12,810	-//-
Declared duplicate reaction					
29	$NNH+H=N_2+H_2$	1.00E+14	0	0	-//-
30	$NNH+N=NH+N_2$	3.00E+13	0	8370	-//-
31	$NNH+NH=N_2+NH_2$	2.00E+11	0.5	8370	-//-
32	$NNH+NH_2=N_2+NH_3$	1.00E+13	0	0	-//-
33	$NNH+NNH=N_2H_2+N_2$	1.00E+13	0	16,750	-//-

TABLE 1: Continued

Number	Reaction	*A*	*n*	E_a	Reference
34	$N_2H_2+M=NNH+H+M$	5.00E+16	0	209,340	-//-
Enhanced third-body efficiency: N_2=2.0; H_2=2.0					
35	$N_2H_2+M=NH+NH+M$	3.16E+16	0	416,170	-//-
Enhanced third-body efficiency: N_2=2.0; H_2=2.0					
36	$N_2H_2+H=NNH+H_2$	8.50E+04	2.6	−963	-//-
37	$N_2H_2+N=NNH+NH$	1.00E+06	2	0	-//-
38	$N_2H_2+NH=NNH+NH_2$	1.00E+13	0	25,120	-//-
39	$N_2H_2+NH_2=NH_3+NNH$	8.80E−02	4	−6740	-//-
40	$N_2H_3+M=NH_2+NH+M$	5.00E+16	0	251,210	-//-
41	$N_2H_3+M=N_2H_2+H+M$	1.00E+17	0	138,160	-//-
42	$N_2H_3+H=N_2H_2+H_2$	1.00E+13	0	0	-//-
43	$N_2H_3+H=NH_2+NH_2$	5.00E+13	0	8370	-//-
44	$N_2H_3+H=NH+NH_3$	1.00E+11	0	0	-//-
45	$N_2H_3+N=N_2H_2+NH$	1.00E+06	2	0	-//-
46	$N_2H_3+NH=N_2H_2+NH_2$	2.00E+13	0	0	-//-
47	$N_2H_3+NH_2=N_2H_2+NH_3$	1.00E+11	0.5	0	-//-
48	$N_2H_3+NNH=N_2H_2+N_2H_2$	1.00E+13	0	16,750	-//-
49	$N_2H_3+N_2H_3=NH_3+NH_3+N_2$	3.00E+12	0	0	-//-
50	$N_2H_3+N_2H_3=N_2H_4+N_2H_2$	1.20E+13	0	0	-//-
51	$N_2H_4(+M)=NH_2+NH_2(+M)$	5.00E+14	0	251,210	-//-
Low pressure limit: 1.50E+15; 0.00E+00; 1.63E+05					
Enhanced third-body efficiency: N_2=2.4; NH_3=3.0; N_2H_4=4.0					
52	$N_2H_4+M=N_2H_3+H+M$	1.00E+15	0	266,280	-//-
Enhanced third-body efficiency: N_2=2.4; NH_3=3.0; N_2H_4=4.0					
53	$N_2H_4+H=N_2H_3+H_2$	7.00E+12	0	10,470	-//-
54	$N_2H_4+H=NH_2+NH_3$	2.40E+09	0	12,980	-//-
55	$N_2H_4+N=N_2H_3+NH$	1.00E+10	1	8370	-//-
56	$N_2H_4+NH=NH_2+N_2H_3$	1.00E+09	1.5	8370	-//-
57	$N_2H_4+NH_2=N_2H_3+NH_3$	1.80E+06	1.7	−5780	-//-
58	$N_3+N_3=N_2+N_2+N_2$	8.43E+11	0	0	NIST
59	$H+N_3=N_2+NH$	6.03E+13	0	0	-//-
60	$N_3+N=N_2+N_2$	8.43E+13	0	0	-//-

cients of structurally similar C–N compounds and the thermodynamic parameters were taken from Burcat (2006). Calculations were performed using the PREMIX, EQUIL, and SENKIN codes from the CHEMKIN-II package (Kee et al., 1989). The size of the calculated area in the PREMIX code was from −5 to 15 (in some calculations, 50 or 100) cm. Temperature increase by 400 K was used as the criterion for the time of the ignition delay in the SENKIN code.

The mechanism contains five reactions with the participation of the HN_3 molecule. Reaction R1 (HN_3+M→NH+N_2+M) is the most important reaction in the proposed mechanism because it determines the flame propagation velocity (Rozenberg et al., 1970). The following is a discussion of the different temperature dependences of the rate constant of reaction R1 derived from the experimental data and from the computational results.

Thermal decomposition of HN_3 can proceed to form NH in the ground (triplet) and the excited (singlet) state. In this study, the two-channel thermal decomposition of hydrogen azide was studied computationally. A model of the reaction was created on the basis of the theoretical study of the reaction potential energy surface and microscopic reaction rates by Besora and Harvey (2008) and the experimental data on the energy-dependent rate constants reported by Foy et al. (1989, 1990). Pressure- and temperature-dependent rate constants of HN_3 decomposition were calculated via solution of a steady-state master equation (Gilbert and Smith, 1990) using the Nesbet algorithm (Gaynor et al., 1978). The exponential-down (Gilbert and Smith, 1990; Holbrook et al., 1996) model of collisional energy transfer was used in the calculations. The values of the critical energy transfer parameter, $\left\langle \Delta E_{\text{down}} \right\rangle$, was adjusted based on agreement with the experimental $k\left(T,P\right)$ data of Röhrig and Wagner (1994) performed in argon bath gas. The model of HN_3 used is based on the vibrational frequencies by Shimanouchi (1972). The collisional energy transfer parameter is unknown for N_2 and HN_3. Thus, the value of this parameter for N_2 was taken as equal to that used for argon (349 cm^{-1}). It is possible that the value for N_2 can be somewhat larger, but it is unlikely that it will be more than a factor of 1.5 larger. For the collisions between HN_3 and HN_3, due to the observed strong dependence of the flame speed on the concentration of HN_3 in the mixture, $\left\langle \Delta E_{\text{down}} \right\rangle$ equal to 2000 cm^{-1} was taken as a possible upper limit. Since the triplet pathway is dominant in the thermal decomposition of hydrogen azide, the contribution of the singlet pathway was neglected. For the purpose of comparative analysis of the performance of the mechanism, the following calculated temperature dependences of the rate constant of reaction R1 at 50 Torr pressure were used (corresponding to different bath gases M):

$$k_{1,6} = 2.88\times10^{35}\times T^{-5.81}\times\exp\left(-25150/T\right),\quad \mathrm{M}=\mathrm{Ar} \tag{1}$$

$$k_{1,7} = 3.73\times10^{35}\times T^{-5.81}\times\exp\left(-25237/T\right),\quad \mathrm{M}=\mathrm{N_2} \tag{2}$$

$$k_{1,8} = 8.93\times10^{34}\times T^{-5.28}\times\exp\left(-26190/T\right),\quad \mathrm{M}=\mathrm{HN_3} \tag{3}$$

where the units are mol, cm, and K.

Figure 1 presents a comparison between different approximations to the temperature dependence of the rate constant of reaction R1 between 1000 and 4000 K. The lines and the curves indexed as $k_{1,1}$–$k_{1,5}$ correspond to the dependences derived from the corresponding experiments listed in the caption; those denoted as $k_{1,6}$, $k_{1,7}$, and $k_{1,8}$ are the results of the calculations (see above) performed for the dominant, triplet channel of HN_3 decomposition in different bath gases (Ar, N_2, and HN_3).

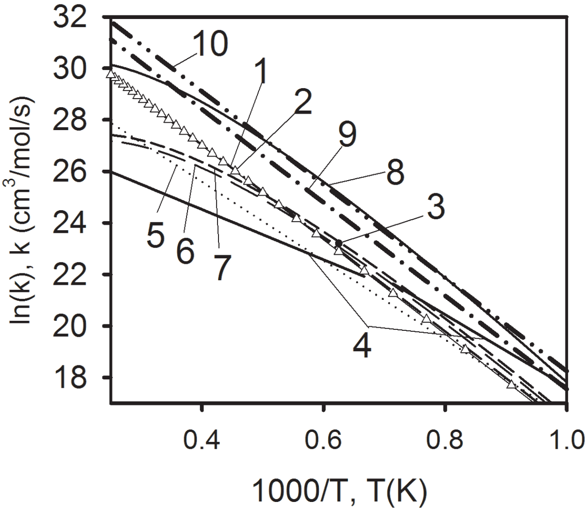

FIG. 1: Arrhenius dependences of the rate constant of reaction R1: HN_3+M=N_2+NH+M. Notations: (1) $k_{1,1} = k_{\mathrm{eff}}$, M=Ar (Kajimoto et al., 1979); (2) $k_{1,2}$, M=Ar (Rohrig and Wagner, 1994); (3) $k_{1,3}$ (Zaslonko et al., 1972); (4) $k_{1,4}$ (Pillard et al., 1985); (5) $k_{1,5}$, M=Ar, triplet (Kajimoto et al., 1979); (6) $k_{1,6}$, triplet, M=Ar, calculation; (7) $k_{1,7}$, triplet, M=N_2, calculation; $k_{1,8}$, triplet, M=HN_3, calculation; $k_{1,9} - 4 \times k_{\mathrm{eff}}$, M=$N_2$, this study; $k_{1,10} - 8 \times k_{\mathrm{eff}}$, M=$HN_3$, this study. Additional notations: (triplet) HN_3 decomposition with formation of 3NH; (calculation) this study; (M) diluent type (bath gas).

It can be seen from Fig. 1 that the experimental values reported by three different groups in the temperature range of 1200–2000 K and pressures of 55–2200 Torr of argon bath gas, $k_{1,1}$ (Kajimoto et al., 1979), $k_{1,2}$ (Röhrig and Wagner, 1994), and $k_{1,3}$ (Zaslonko et al., 1972), can be reasonably described with one temperature dependence, $k_{\mathrm{eff}}(T)$. Therefore, to describe the rate constant of reaction R1 (HN_3+Ar→HN+N_2+Ar) for the entire temperature range in the proposed mechanism, an approximation of $k_{\mathrm{eff}} = k_{1,1}$ (Fig. 1) was selected. Here, the quantum states of NH were not distinguished and potential reactions of the excited-state NH were not considered.

The purpose of the current study is to develop a mechanism that would adequately describe all existing experimental data for HN_3 mixtures with different diluents (N_2, Ar, and He bath gases) and different HN_3 concentrations, ranging from 25% to 100%.

As noted above, the experiments of Dupre et al. (1976) and Meyer and Schumacher (1934) appear to have been strongly influenced by the effects of the reactor vessel walls on the results of the measurement. To avoid complications due to unknown wall effects, first the mechanism was tested for the flame propagation velocity, where the influence of the walls is absent. To ensure adequate description of the experimental data by the calculated flame speed, third-body efficiency coefficients were introduced for R1: 1 for Ar, 4 for He and N_2, and 8 for HN_3. Figure 1 shows that the calculated $k_{1,6}$ values for the triplet pathway of the reaction are ~2–3 times higher than the experimentally obtained values of $k_{1,5}$ in the ~1250–2500 K range of temperatures; they reasonably agree with the $k_{1,1}$ approximation at temperatures below 2200 K. At temperatures above 2200 K, the $k_{1,1}/k_{1,6}$ ratio increases.

For the HN_3 bath gas, the calculated $k_{1,8}$ values reasonably agree with the proposed $k_{1,10}$ approximation in the temperature range of 1000–2200 K; then, they become lower than $k_{1,1}$ as the temperature grows. For the N_2 bath gas, the $k_{1,9}$ rate constant values used in the proposed mechanism exceed the calculated values of $k_{1,7}$ by a factor ranging from ~3 to 12. Rate constants for reactions R2 and R3 with participation of HN_3 were taken from Le Bras and Combourieu (1973). Reactions R6–R57 and their rate constants (Konnov and De Ruyck, 2000, 2001), represent a complete mechanism of hydrazine decomposition, which also includes a mechanism of ammonia decomposition as a subset. Reactions R58–R60 with participation of the N_3 species were taken from the NIST Kinetics Database (NIST, 2008).

2.2 The Velocity of HN_3 Flame Propagation

Figure 2 presents a comparison of the experimental data on the velocity of HN_3 flame propagation (S_u) with the results of calculations performed using the mechanism developed in the current study (Table 1). Experimental data obtained in three different diluents (Ar, N_2, and He) are shown; dependences on the HN_3 mole fraction are given for Ar and N_2 diluents. For all flames, the initial temperature was 296 K and the overall pressure was 50 Torr.

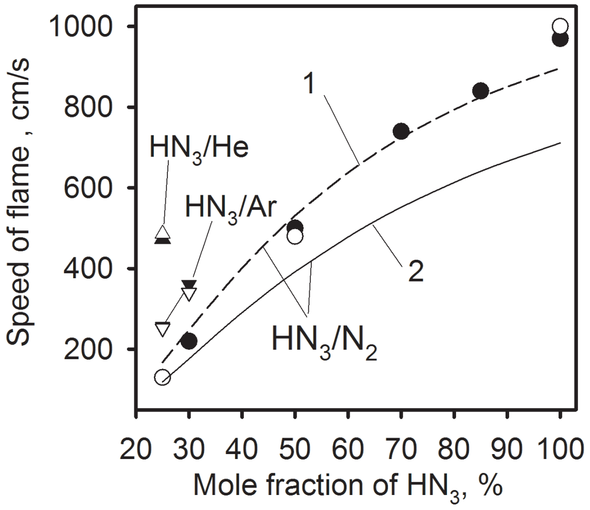

FIG. 2: Speed of flame in HN_3 mixtures with different diluents at $p = 50$ Torr, $T_0 = 296$ K. Diluent N_2: Line 1, modeling using $k_{1,1}$, $k_{1,9}$, and $k_{1,10}$; Line 2, modeling using $k_{1,6}$, $k_{1,7}$, and $k_{1,8}$; symbols ● and ○, experiment (Laffitte et al., 1965; Combourieu, 1966); diluent Ar (modeling, ∇; experiment, ▼ (Combourieu, 1966); diluent He (modeling, Δ; experiment, ▲ (Combourieu, 1966).

For reaction R1, effects of different approximations to $k_1(T)$ were considered. Using the calculated $k_{1,6}$, $k_{1,7}$, and $k_{1,8}$ temperature dependences did not result in a good match with the experimental data. Therefore, the $k_{1,6}$, $k_{1,7}$, and $k_{1,8}$ dependences were not used in the proposed mechanism. At the same time, using $k_{1,1}$, $k_{1,9}$, and $k_{1,10}$ resulted in satisfactory agreement between the experimental and the computed data on the flame speed for the entire range of HN_3 concentrations in the mixture with nitrogen, as well as for other types of diluents (Ar, He). The free flame propagation velocity increased from ~1.2 m/s^{-1} to ~10 m/s^{-1} with the concentrations of HN_3 in nitrogen changing from 25% to 100%. Introduction of a third-body efficiency coefficient for N_2 allowed us to obtain the values of free propagation velocity for the HN_3/N_2 mixture that are in agreement with the experimental data (Laffitte et al., 1965) at high diluent concentration. Introduction of a third-body efficiency coefficient for HN_3 allowed us to obtain a satisfactory agreement at low diluent concentration, as well as under the conditions of 100% HN_3. Similarly, satisfactory agreement with the experimental flame propagation velocities was obtained for other diluents: Ar and He.

Existing literature data indicate that ~25% is the lowest concentration of HN_3 in nitrogen in which self-ignition and flame propagation are possible (Rozenberg et al., 1970). Modeling flame self-ignition and propagation with the proposed mechanism demonstrated that with a 20% HN_3 concentration a solution cannot be obtained.

It was shown by Laffitte et al. (1965) that the flame speed of HN_3 does not depend on pressure. A similar result was obtained in modeling using the developed mechanism. As the pressure increased from 50 to 500 Torr, the flame speed in the 85% HN_3+15% N_2 mixture did not change: the corresponding values were 825 and 823 cm/s^{-1}, respectively.

A sensitivity analysis of the flame propagation velocity performed with the proposed mechanism demonstrated strong dependence of the flame speed on the rate constant of reaction R1. The relative change in the flame speed reached 25% if the rate constant of reaction R1 was changed by a factor of 5. The rate constants of reactions R18, R13, and R3 exerted 5–6 times less influence.

Thus, the proposed mechanism (Table 1) adequately describes a wide range of experimental data related to the flame speed of HN_3.

2.3 Structure of HN_3 Flames with Different Degrees of N_2 Dilution

Figures 3 and 4 display the results of modeling of the flame structure with different HN_3/N_2 ratios: 0.3/0.7 (F1) and 0.85/0.15 (F2). Computations were performed with $T_0 = 296$ K and $P = 50$ Torr using the PREMIX code and the proposed mechanism (Table 1). Shown in the Figs. 3 and 4 are the concentration profiles of the major and the intermediate species: H_2, N_2, NH_3, NH_2, NH, N, and H. Here, NH_3 is the intermediate species that appears first in both flames. Its maximum concentration was reached at $T \approx 1500$ K. The concentration profiles of N_xH_y species pass through their respective maxima in the following sequence: NH_3, NH_2, NH, and N.

It is likely that the bright yellow luminosity observed in the experiment (Laffitte et al., 1965) is caused by the intermediate products. The width of the flame zone deter-

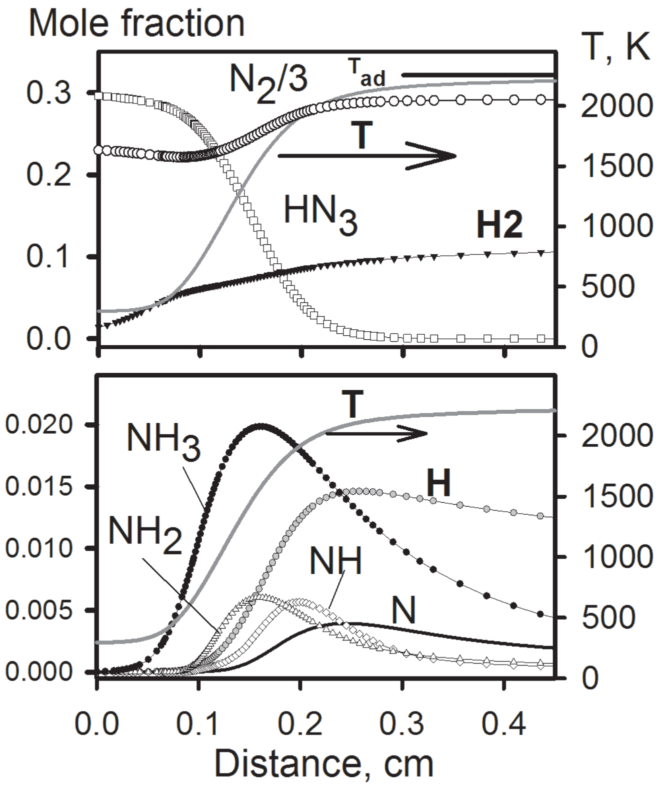

FIG. 3: Flame structure of the 0.3/0.7 HN_3/N_2 mixture with $T_0 = 296$ K at $P = 50$ Torr

mined by the distance of complete consumption of HN_3 (~0.3 cm for F1 and ~0.12 for F2) decreased by a factor of ~2.5 as the HN_3 initial concentration in the mixture was increased from 0.3 to 0.85 mole fraction. This effect is in agreement with the similar reduction (a factor of ~2.5) of the width of the luminous flame zone in the experimental study of Laffitte et al. (1965).

According to the modeling results, the main intermediate products in flame F1 that may be responsible for the flame luminosity are NH_3, NH_2, and NH. In the studies done by Hall and Wolfhard (1956), Eckl and Eisenreich (1992), and Yamasaki et al. (1993), where the emission spectra for NH, NH_2, and NH_3 were measured, it was determined that NH and NH_3 have emission lines in the invisible spectral ranges: 330.1 and 336 nm for NH and a wide line in the IR region for NH_3; NH_2 emits light in the visible range of the spectrum. One of the maxima in its emission spectrum is at a wavelength of 575 nm (Yamasaki et al., 1993), which corresponds to the yellow color. It can be suggested that the experimentally observed luminous zone in the HN_3 flame is caused by the emission of a NH_2 radical. For example, according to the modeling results, for flame F1 the

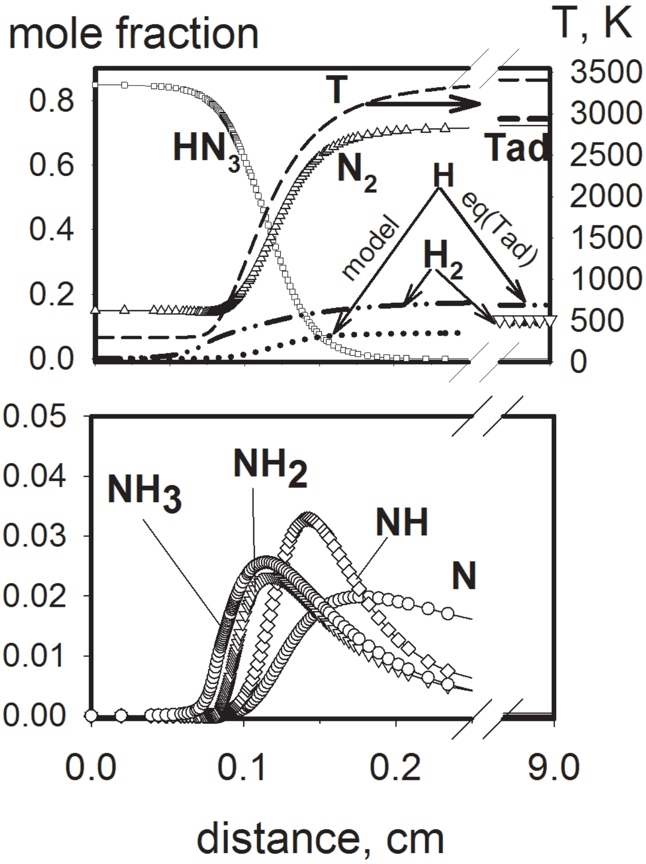

FIG. 4: Flame structure of the 0.85/0.15 HN3/N2 mixture with $T_0 = 296$ K at $P = 50$ Torr

width of the NH_2 profile is 0.1 cm, which exceeds the luminous zone in a similar flame by approximately a factor of 2 (Laffitte et al., 1965). Such agreement may be considered satisfactory.

The modeling results indicate that for flame F1 (Fig. 3) the maximum temperature does not exceed the adiabatic value within the area covered by the calculations for this mixture (~15 cm) and it is reached at a considerable distance from the origin of coordinates (~50 cm). The composition of the final combustion products corresponds to thermodynamic equilibrium.

As opposed to flame F1, in the case of flame F2 (Fig. 4) the maximum value of the temperature in the flame front ($T_{\text{fl}}^{\max}$) exceeds its adiabatic value (T_{ad}). In the literature, this phenomenon is known as the "super adiabatic flame temperature" (SAFT) (Bertagnolli and Lucht, 1996; Liu and Gülder, 2008a,b). Table 2 demonstrates the species composition (in mole fractions) and temperature in flame F2 at a distance of 1.5 cm from the origin of the coordinates. Figure 4 shows the same at a distance of 9 cm, with comparison to thermodynamic equilibrium values. It can be seen that already at the distance of 1.5 cm, practically all of the nitrogen-containing species and radicals have been consumed. The mass fraction of nitrogen (0.725×28/20.77) coincides with its value at T_{ad} (0.7×28/20.03).

TABLE 2: Composition (in mole fractions) and temperature in the $0.85HN_3/0.15N_2$ flame (F2)

	N_2	H_2	H	NH	NH_3	NH_2	MW	*T* (K)
PREMIX (1.5 cm)	0.725	0.172	0.1	5.3×10^{-4}	5×10^{-5}	1.3×10^{-4}	20.77	3433
Equilibrium	0.7	0.121	0.176	1.5×10^{-6}	1.7×10^{-8}	8.8×10^{-8}	20.03	2940

Thus, it is observed that nitrogen-containing species in the HN_3 flame achieve their thermodynamic equilibrium concentrations. It also can be seen that the difference between the equilibrium composition of the mixture and the actual one (Table 2, Fig. 4) is in concentrations of H_2 and H. In the case of the F2 flame, the calculated H_2 concentration exceeds its thermodynamic equilibrium value. At a distance of 100 cm from the flame front (in the post-flame zone), the temperature decreases by ~290 K and the concentrations of H_2 and H approach their equilibrium values (Fig. 5). Increasing the size of the calculated area will most likely result in a further reduction of the temperature to its adiabatic value. As demonstrated by kinetic analysis of the reaction mechanism, the rate of approach to equilibrium is determined by the reaction kinetics and, in particular, by that of the recombination/decomposition reaction $H+H+M=H_2+M$. The rate of this reaction depends on the pressure and is rather low at a low pressure of 50 Torr. It should be noted that broadening of the area covered by the calculations does not affect the flame propagation velocity and the amount by which the flame temperature exceeds the adiabatic temperature of the mixture.

Table 3 demonstrates the maximum temperature values in the flame front (T_{fl}^{max}) obtained by modeling the flame structure in comparison with the adiabatic values (T_{ad}) for mixtures with different HN_3 compositions (nitrogen diluent) at a pressure of 50 Torr. Analysis of these data shows that the maximum temperature values in the flame front exceed the adiabatic values by 40–610°, if the HN_3 concentration in the mixture is larger than 40%. In the case of a mixture of HN_3 with Ar, SAFT is observed already with 30% HN_3. Therefore, it can be concluded that the SAFT phenomenon, well-known for hydrocarbon flames (Bertagnolli and Lucht, 1996), is also observed in this study of HN_3 flames.

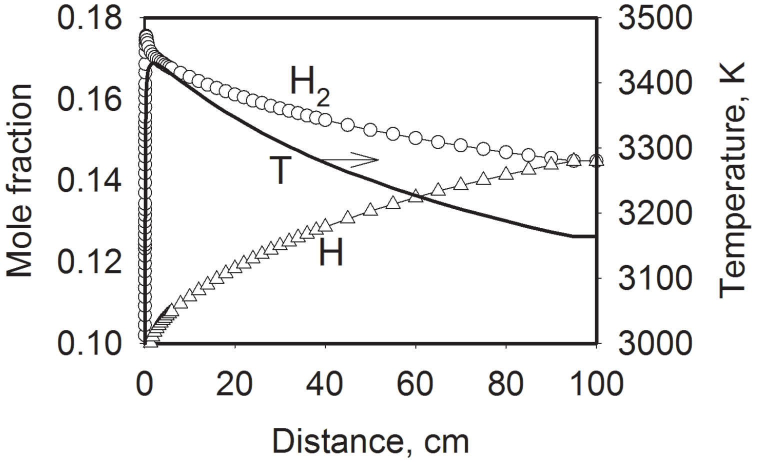

FIG. 5: Post-flame zone of the 0.85/0.15 HN_3/N_2 mixture at $T_0 = 296$ K and $P = 50$ Torr

TABLE 3: Comparison of the maximum temperature values in the flame front ($T_{\text{fl}}^{\text{max}}$) obtained by modeling the flame structure with the adiabatic values (T_{ad}) for mixtures with different fractions of HN_3 in nitrogen at 50 Torr pressure

HN_3 (%)	30	40	50	85	100
$T_{\text{fl}}^{\text{max}}$ (K)	2257[1]	2563	2819	3433	3610
T_{ad} (K)	2257	2522	2677	2939	2998
$T_{\text{fl}}^{\text{max}} - T_{\text{ad}}$ (K)	0	41	142	494	612

[1] Modeling up to ~50 cm.

2.4 Self-Ignition Limits of HN_3

Figure 6 displays the self-ignition limits (pressure and temperature) of HN_3 determined experimentally in a static reactor (Gray, 1957); the corresponding induction period (τ_{ind}) was ~0.2 s. The dependence of the limiting pressure for self-ignition of HN_3 on temperature [$P_{HN_3}(T)$] calculated using the proposed mechanism and the same value of the induction period differs from the experimentally determined curve (Fig. 6). One potential reason for the difference may be the low accuracy in measuring τ_{ind} in the

Gray (1957) experiments; the actual τ_{ind} values may be lower than 0.2 s. The modeling results coincide with the experimental data at $\tau_{\mathrm{ind}} \sim 10^{-2}$–$10^{-3}$ s. Thus, it can be concluded that the proposed mechanism results in a semi-quantitative description of the $P_{\mathrm{HN}_3}(T)$ dependence.

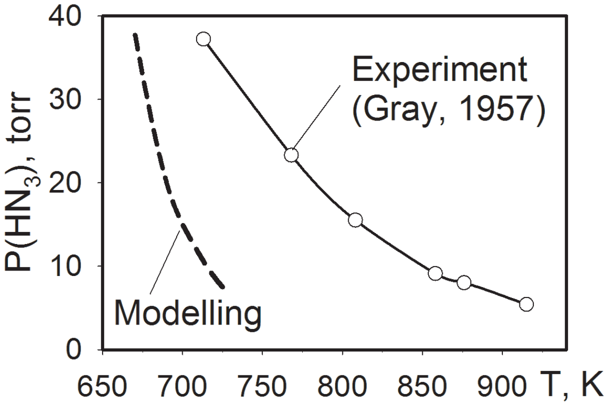

FIG. 6: Self-ignition limits for HN_3: experiment (Gray, 1957) and modeling ($\tau_{\mathrm{ind}} \sim 0.2$ s)

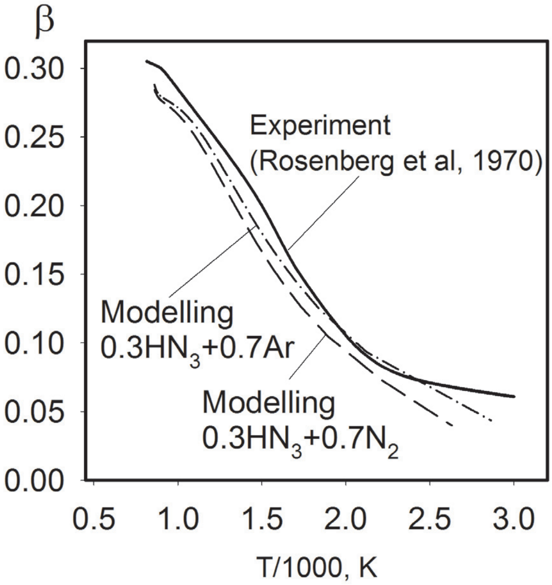

FIG. 7: Temperature dependence of the relative yield of NH_3 (β) in the ignition products of HN_3 mixtures with different diluents at low pressure

Figure 7 presents the results of modeling of the temperature dependence of the relative yield of NH_3 (β) during the ignition of HN_3 mixed with different diluents (Ar and N_2) at a pressure of 50 Torr. Here, $\beta = (NH_3) / \left[(HN_3)^0 - (HN_3) \right]$, where ($NH_3$), ($HN_3$), and $(HN_3)^0$ are the current and the initial concentrations of the corresponding species. As can be seen from the plot in Fig. 7, these data adequately describe the experimental results of Rozenberg et al. (1970).

3. CONCLUSION

A kinetic mechanism of the combustion of HN_3 has been developed. The mechanism adequately describes the experimental results on flame propagation velocity and on self-ignition limits of mixtures containing HN_3. Modeling of the flame structure of HN_3-containing mixtures at a pressure of 50 Torr demonstrates the occurrence of the phenomenon of SAFT. The developed mechanism can be used to describe combustion and thermal decomposition in chemical systems containing HN_3.

REFERENCES

Alexander, M. H., Werner, H.-J., Hemmer, T., and Knowles, P. J., Ab initio study of the energetic of the spin-allowed and spin-forbidden decomposition of HN_3, *J. Chem. Phys.*, vol. **93**, no. 5, pp. 3307–3318, 1990.

Bertagnolli, K. E. and Lucht, R. P., Temperature profile measurements in stagnation-flow, diamond-forming flames using hydrogen CARS spectroscopy, *Proc. of 26th International Symposium on Combustion*, vol. **26**, pp. 1825–1833, 1996.

Besora, N. and Harvey, J. N., Understanding the rate of spin-forbidden thermolysis of HN_3 and CH_3N_3, *J. Chem. Phys.*, vol. **129**, no. 4, pp. 044303-1–044303-10, 2008.

Burcat, A., Thermodynamic data, Laboratory for Chemical Kinetics, Institute of Chemistry, Eotvos University (ELTE), Budapest, Hungary, retrieved August 14, 2008 from http://garfield.chem.elte.hu/Burcat/burcat.html, 2006.

Dupre, G., Paillard, C., and Combourieu, J., Study of the decomposition flame of gaseous azides by time-of-flight mass spectrometry, in *Dynamic Mass Spectrometry*, eds., Price, D. and Todd, J. F. J., vol. **4**, pp. 233–245, London: Heyden, 1976.

Eckl, W. and Eisenreich, N., Determination of the temperature in a solid propellant flame by analysis of emission spectra, *Propellants, Explos., Pyrotech*, vol. **17**, pp. 202–206, 1992.

Foy, B. R., Casassa, M. P., Stephenson, J. C., and King, D. S., Dissociation lifetimes and level mixing in overtone-excited HN_3, *J. Chem. Phys.*, vol. **90**, no. 12, pp. 7037–7045, 1989.

Foy, B. R., Casassa, M. P., Stephenson, J. C., and King, D. S., Overtone-excited HN_3: Anharmonic resonance, homogeneous line widths, and dissociation rates, *J. Chem. Phys.,* vol. **92**, no. 5, pp. 2782–2789, 1990 .

Gaynor, B. J., Gilbert, R. G., and King, K. D., Solution of the master equation for unimolecular reactions, *Chem. Phys. Lett.*, vol. **55**, no. 1, pp. 40–43, 1978.

Gilbert, R. G. and Smith, S. C., *Theory of Unimolecular and Recombination Reactions*; Oxford, UK: Blackwell, 1990.

Gray, P., Spontaneous ignition of gaseous hydrogen azide, *Nature,* vol. **179**, no. 4559, pp. 576–577, 1957.

Hajal, I. and Combourieu, J., Analyse theorique de quelques caracteristiques experimentales de la deflagration de l'acide azothydrique gazeux, *J. Chim. Phys.*, vol. **63**, no. 6, pp. 899–905, 1966.

Hall, A. R. and Wolfhard, H. G., Hydrazine decomposition flames at subatmospheric pressures, *Trans. Faraday Soc.,* vol. **52**, pp. 1520–1525, 1956.

Holbrook, K. A., Pilling, M. J., and Robertson, S. H., *Unimolecular Reactions*, 2nd ed., New York: Wiley, 1996.

Kajimoto, O., Yamamoto, T., and Fueno, T., Kinetic studies of the thermal decomposition of hydrazoic acid in shock waves, *Phys. Chem*., vol. **83**, no. 4, pp. 429–435, 1979.

Kee, R. J., Rupley, F. M. and Miller, J. A., Chemkin II: A Fortran chemical kinetics package for the analysis of gas-phase chemical kinetics, *Report No. SAND89-8009*, Sandia National Laboratories, 1989.

Konnov, A. A., Detailed reaction mechanism for small hydrocarbons combustion. Release 0.4,

retrieved August 14, 2008, http://homepages.vub.ac.be/~akonnov/science/mechanism/version0_4.html, 1998.

Konnov, A. A. and De Ruyck, J., Kinetic modelling of the thermal decomposition of ammonia, *Combust. Sci. Technol*., vol. **152**, pp. 23–37, 2000.

Konnov, A. A. and De Ruyck, J., Kinetic modelling of the decomposition and flames of hydrazine, *Combust. Flame*, vol. **124**, pp. 106–126, 2001.

Laffitte, P., Hajal, I., and Combourieu, J., The decomposition flame of hydrogen azide, *Proc. of 10th International Symposium on Combustion*, pp. 79–85, 1965.

Le Bras, G. and Combourieu, J., The reactions of atomic hydrogen and active nitrogen with hydrogen azide, *Int. J. Chem. Kinet*., vol. **5**, pp. 559–576, 1973.

Liu, F. and Gülder, Ö. L., Effect of pressure and preheat on super-adiabatic flame temperatures in rich premixed methane/air flames, *Combust. Sci. Technol.*, vol. **180**, pp. 437–452, 2008a.

Liu, F. and Gülder, Ö. L., Effects of H_2 and H preferential diffusion and unity Lewis number on superadiabatic flame temperatures in rich premixed methane flames, *Combust. Flame*, vol. **143**, pp. 264–281, 2008b.

Meyer, R. and Schumacher, H.-J., Uber den nicht explosive verlaufenden thermischen Zerfall der Stickstoffwasserstoffsaure, *Z. Phys. Chem. Abt. A*, vol. **170**, pp. 33–40, 1934.

National Institute of Standards and Technology (NIST), NIST chemical kinetics database, retrieved from http://kinetics.nist.gov/, NIST, 2008.

Pillard, C., Dupre, G., and Combourieu J., Pyrolyses endothermiques gazeux par la methode du tube a choc, *J. Chim. Phys*., vol. **82**, no. 5, pp. 489–497, 1985.

Röhrig, M. and Wagner, H. G., A kinetic study about the reactions of $NH(X^3\Sigma^-)$ with hydrocarbons. Part 1: Saturated hydrocarbons and acetaldehyde, *Ber. Bunsenges. Phys. Chem.*, vol. **98**, no. 6, pp. 858–863, 1994.

Rozenberg, A. S., Arsen'ev, Yu. N., and Voronkov, V. G., Ignition of gaseous mixtures of hydrazoic acid and various diluents, *Combust., Explos. Shock Waves,* vol. **6**, no. 3, pp. 271–277, 1970.

Shimanouchi, T., *Tables of Molecular Vibrational Frequencies. Consolidated Volume I*, Gaithersburg, MD: National Bureau of Standards, 1972.

Yamasaki, K., Watanabe, A., Tokue, I., and Ito, Y., Dispersed emission spectrum of NH_2 in the ultraviolet laser photolysis of HN_3 and the mechanism of formation, *Chem. Phys. Lett.*, vol. **204**, no. 1-2, pp. 106–110, 1993.

Zaslonko, I. S., Kogarko, S. M., and Mozjuchin, E. V., About mechanism of thermal decomposition of hydrazoic acid, *Kinet. Katal.*, vol. **13**, no. 4, pp. 829–835, 1972.